



CLINICAL REPORT

Terminal osseous dysplasia with pigmentary defects and cardiomyopathy caused by a novel *FLNA* variant

Lynne Rumping¹  | Marja W. Wessels² | Alex V. Postma^{1,3} |
 Joost van Schuppen⁴ | Marjon A. van Slegtenhorst² | Jasper J. Saris² |
 J. Peter van Tintelen^{1,5} | Stephen P. Robertson⁶  | Mariëlle Alders¹ |
 Saskia M. Maas¹ | Ronald H. Lekanne Deprez¹

¹Department of Clinical Genetics, Amsterdam UMC, University of Amsterdam, Amsterdam, The Netherlands

²Department of Clinical Genetics, Erasmus Medical Centre, Rotterdam, The Netherlands

³Department of Medical Biology, Amsterdam UMC, University of Amsterdam, Amsterdam, The Netherlands

⁴Department of Radiology and Nuclear Medicine, Amsterdam UMC, University of Amsterdam, Amsterdam, The Netherlands

⁵Department of Genetics, University Medical Center Utrecht, Utrecht, The Netherlands

⁶Department of Women's and Children's Health, University of Otago, Dunedin, New Zealand

Correspondence

Lynne Rumping, Amsterdam University Medical Centre, Location AMC, Clinical Genetics Meibergdreef 9 1105 AZ Amsterdam, The Netherlands.
 Email: l.rumping@amsterdamumc.nl

Abstract

Terminal osseous dysplasia with pigmentary defects (TODPD), also known as digitocutaneous dysplasia, is one of the X-linked filaminopathies caused by a variety of *FLNA*-variants. TODPD is characterized by skeletal defects, skin fibromata and dysmorphic facial features. So far, only a single recurrent variant (c.5217G>A;p.Val1724_Thr1739del) in *FLNA* has found to be responsible for TODPD. We identified a novel c.5217+5G>C variant in *FLNA* in a female proband with skeletal defects, skin fibromata, interstitial lung disease, epilepsy, and restrictive cardiomyopathy. This variant causes mis-splicing of exon 31 predicting the production of a *FLNA*-protein with an in-frame-deletion of 16 residues identical to the miss-splicing-effect of the recurrent TODPD c.5217G>A variant. This mis-spliced transcript was explicitly detected in heart tissue, but was absent from blood, skin, and lung. X-inactivation analyses showed extreme skewing with almost complete inactivation of the mutated allele (>90%) in these tissues, except for heart. The mother of the proband, who also has fibromata and skeletal abnormalities, is also carrier of the *FLNA*-variant and was diagnosed with noncompaction cardiomyopathy after cardiac screening. No other relevant variants in cardiomyopathy-related genes were found. Here we describe a novel variant in *FLNA* (c.5217+5G>C) as the second pathogenic variant responsible for TODPD. Cardiomyopathy has not been described as a phenotypic feature of TODPD before.

KEYWORDS

cardiomyopathy, filaminopathies, *FLNA*, phenotype–genotype correlation, terminal osseous dysplasia with pigmentary defects

Saskia M. Maas and Ronald H. Lekanne Deprez share last authorship.

This is an open access article under the terms of the Creative Commons Attribution-NonCommercial-NoDerivs License, which permits use and distribution in any medium, provided the original work is properly cited, the use is non-commercial and no modifications or adaptations are made.

© 2021 The Authors. *American Journal of Medical Genetics Part A* published by Wiley Periodicals LLC.

1 | INTRODUCTION

Terminal osseous dysplasia with pigmentary defects (TODPD, OMIM #300244) is one of the 10 X-linked filaminopathies caused by pathogenic variants in *FLNA* (Breuning et al., 2000; Brunetti-Pierrri et al., 2010; Horii et al., 1998; Sun et al., 2010; Wade et al., 2020). *FLNA* is widely expressed and its protein structure includes a rod domain of 24 structurally homologous “repeats” many with specific functions as indicated by the phenotypic consequences of missense variants (Wade et al., 2020). Depending on the location of such variants within *FLNA*, a wide spectrum of disorders involving multiple organs with a clear phenotype–genotype correlation have been observed (Robertson, 2005). Loss-of-function variants are mainly associated with periventricular nodular heterotopia (PH) with secondary epilepsy, interstitial lung disease, connective tissue abnormalities and valvular cardiac anomalies (Wade et al., 2020). Gain-of-function variants, those that confer an alteration of some functions mediated by the protein, are associated with otopalatodigital spectrum disorders (OPD-SD) characterized by a skeletal dysplasia, dysmorphic facial features and a variety of organ malformations. Within these OPD-SD there is often clinical overlap, however, overlap with patients carrying *FLNA* loss-of-function variants is exceptional (Wade et al., 2020).

TODPD is part of the OPD-spectrum disorders and is a male-lethal disease with X-linked dominant inheritance, characterized by skeletal dysplasia with brachydactyly, camptodactyly, limb deformities, scoliosis, pectus excavatum, and shortened and bowed long bones. Dysmorphic features include recurrent digital fibromata during infancy, multiple frenulae and pigmentary changes of the skin, hypertelorism, colobomata, and short stature (Bhabha et al., 2016; Sun et al., 2010). Only one single recurrent variant (c.5217G>A) in the *FLNA*-gene is known to be responsible for TODPD (Sun et al., 2010). Here, we describe the clinical and molecular evaluation of two patients, a daughter (proband) and mother, with TODPD exhibiting an extended phenotype and a novel c.5217+5G>C variant in *FLNA*.

2 | METHODS

2.1 | Genetic workup

Genomic DNA was obtained from peripheral blood lymphocytes from both the proband and mother according to standard protocols. Genomic DNA isolation from skin, lung and heart tissue from the proband obtained at autopsy was performed with a standard protocol using a Maxwell RSC isolation machine and the Maxwell Tissue isolation kit (Cat no. AS1030). Targeted Sanger sequencing of the *FLNA*-gene was performed according to standard protocols. Additionally, trio-based whole-exome sequencing (WES; 150 bp) with parents—focused on genes associated with cardiomyopathy and the HPO-terms “cardiomyopathy” and “restrictive cardiomyopathy”—was performed on a NextSeq sequencer platform (Illumina) with a coverage of $\times 20$ at greater than 95% of the sequences.

2.2 | RNA analysis

Total RNA was obtained from peripheral blood using PAXgene tubes and the PAXgene blood RNA kit (Qiagen). In addition, total RNA was isolated from skin, lung, and heart tissue from the proband, obtained postmortem. Tissue was homogenized in Trizol reagent (Invitrogen) using a MagNa Lyser Green Beads (Roche). After homogenization Trizol was removed from the tube and used in the standard Trizol RNA extraction protocol. cDNA was produced by reverse transcription-PCR with use of Superscript III kit (Invitrogen). PCRs were performed using *FLNA* specific primer sequences located on the transition of exon 29 and 30 (ACAGTGTCATCGGAGGTCA) and in exon 32 (TGGGCGTAGGTGTACTGTG; Merck Sigma-Aldrich). Sequencing of the cDNA was performed with the Brilliant Dye Terminator Cycle Sequencing system (ThermoFisher Scientific) and Big Dye Terminator kit (Applied Biosystems) and analyzed using CodonCode Aligner version 8.0.2.

2.3 | X-chromosome inactivation analysis

The X-chromosome inactivation pattern was tested with the HUMARA (human androgen receptor gene) assay as described by Allen et al. (1992) using the methylation-sensitive restriction enzymes (HhaI and HpaII). The highly polymorphic CAG trinucleotide repeat in exon 1 of the AR gene (Xq12) was amplified with and without prior methylation-sensitive restriction enzyme digestion. PCR products were run on an ABI3100 sequencer (ThermoFisher Scientific) and results were analyzed using the software Genemapper v5 (ThermoFisher Scientific). Degree of skewing was calculated by quantification as previously described (Lau et al., 1997). X-inactivation was considered skewed when the ratio between the alleles was more than 90:10.

3 | RESULTS

3.1 | Case report

The proband was a 5-year-old girl, the first child of non-consanguineous parents. The pregnancy was uncomplicated. She was born by sectio caesarea because of a narrow shaped pelvis of mother. Her birthweight was 2290 g at 39 weeks ($< -2.5SD$). Cognitive and motor milestones were normal: she sat at 8 months, walked at 11 months and was raised bilingual without problems. At the age of 6 months she presented for the first time with multiple digital fibromata, oral frenulae, and skeletal anomalies of the hands including bilateral hypoplasia of metacarpals 1 and 2, bilateral brachydactyly of the phalanges of digit II, and camptodactyly of the distal phalanx of digit III (Figure 1(a–c)). She had additional dysmorphic features, including short stature ($< -2.5SD$ and $< -1.5SD$ of target height) and low weight ($< -2.5SD$); translucent skin, sparse hair, mild hypertelorism and a prominent forehead. Based on these clinical features

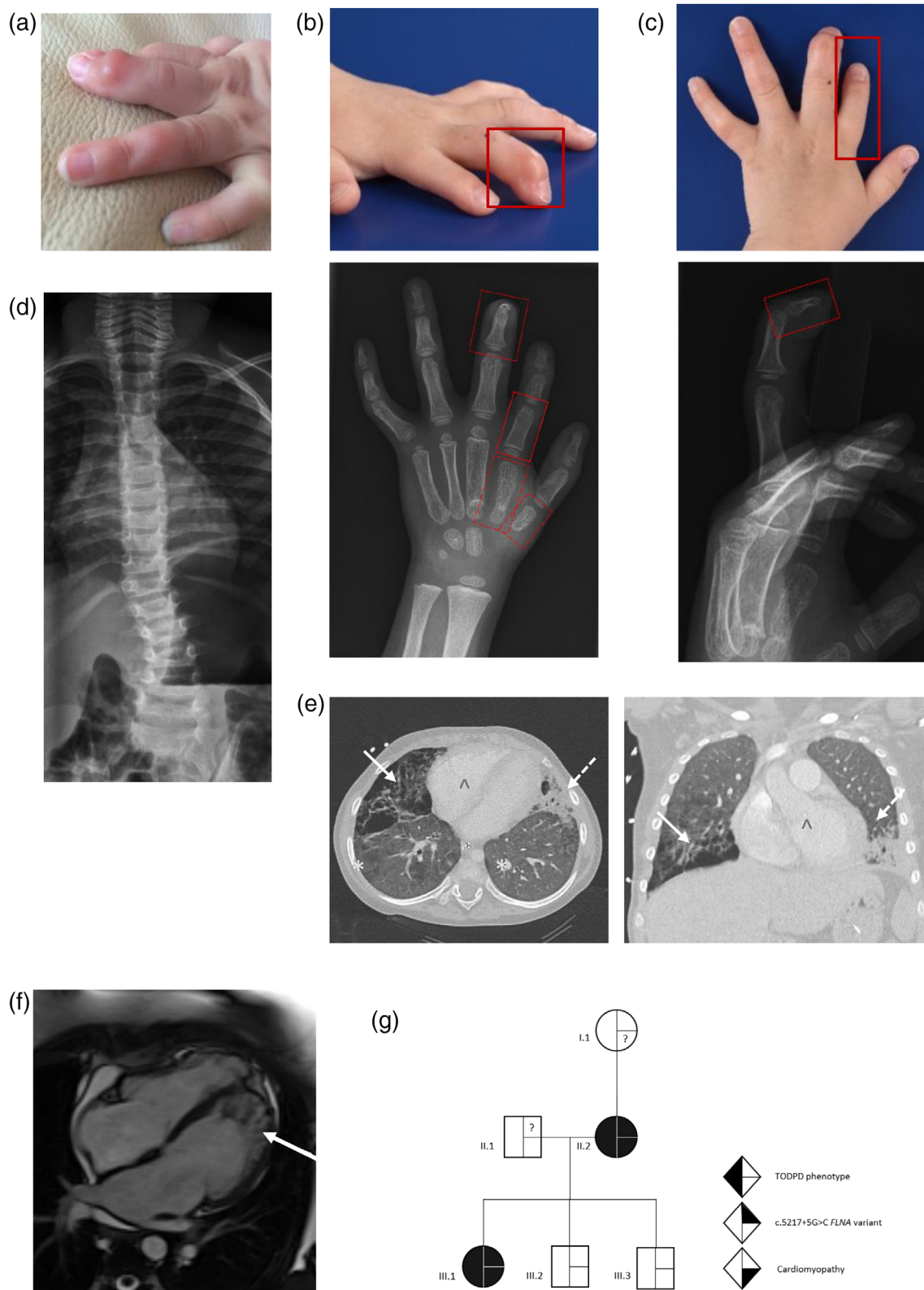


FIGURE 1 Legend on next page.

TODPD was suspected, but could not be confirmed as the single recurrent variant for TODPD c.5217G>A in *FLNA* was not found with Sanger sequencing. However, a *FLNA* variant of unknown significance c.5217+5G>C was detected. At age 2 years, lumbar scoliosis was diagnosed (Figure 1(d)) a sign commonly reported in patients with TODPD. At age 3 years 10 months, she unexpectedly presented at the intensive care unit with severe heart failure due to restrictive cardiomyopathy with severe diastolic and mild systolic dysfunction and dilated atria and ventricles. Mild mitral valve insufficiency was present, without structural abnormalities of the valves. The aorta had a normal diameter. WES-trio analyses with proband and parents—including filtering for genotypes that could mediate an autosomal recessive and dominant, de novo, and X-linked disorder—yielded no other candidates for a cardiomyopathy phenotype. At age 4 years she developed respiratory distress with low CRP levels. CT of the chest revealed bilateral signs of interstitial lung disease, including ground-glass opacities throughout the lungs, fibrotic changes, with bullae, bronchiectasis basal, and middle lobes, with destruction of lung parenchyma (Figure 1(e)). At age 5 years, she presented twice with tonic seizures which spontaneously stopped after few minutes and responded to levetiracetam treatment. Cerebral imaging to exclude PH was planned, but shortly after she deceased from heart failure. Autopsy revealed severe air retention of the basal lung lobes confirming emphysema or lung bullae, no signs of inflammation were observed. The heart weight was increased weight (95 g ref: 72–98 g) with bilateral dilated atria and ventricles and extensive fibroelastosis. Autopsy of the brain was not performed on request of the parents.

The two healthy brothers and the father of the proband did not show any signs of TODPD and echocardiography showed no signs of cardiomyopathy. Segregation analysis revealed absence of the c.5217+5G>C variant in *FLNA* in all three. The mother of the proband was carrier of the c.5217+5G>C *FLNA* variant and was diagnosed with noncompaction cardiomyopathy (noncompaction to compaction layer thickness ratio of 2.8:1 at end diastole; Figure 1(f)). She had multiple digital fibromata in infancy which were surgically removed and has multiple oral frenulae, unilateral camptodactyly of digit III, and short stature (1.43 m [$<-4.4SD$ and $<-3.3SD$ of target height]). The maternal grandmother did not carry the variant, suggesting that variant had occurred de novo in the mother of the proband (Figure 1(g)). It is unknown whether the maternal grandmother and mother's sisters and half-sisters (same mother) have cardiomyopathy, as cardiac screening has not been performed. As far as could be ascertained, there are no

other family members with clinical features of TODPD or cardiomyopathy.

3.2 | Identification of the c.5217+5G>C p.Val1724_Thr1739del *FLNA* variant

Sanger sequencing of *FLNA* revealed the NM_001110556.2:c.5217+5G>C variant (Figure 2(a)). This noncoding *FLNA*-variant has not been associated with TODPD or other human disease before and is absent in 179,736 reference alleles from gnomAD (Lek et al., 2016) and in ClinVar (Landrum et al., 2018). In silico prediction software (SpliceSiteFinder-like, MaxEnsScan, NNSPLICE, and GeneSplicer) all predict the variant to functionally affect transcript splicing. RNA analyses by RT-PCR of *FLNA* transcripts revealed normal splicing in blood. Only after the proband deceased, a RNA mis-splicing effect (r.5170_5217del) could be observed in heart tissue: the variant results in an in-frame deletion of 16 residues (p.Val1724_Thr1739del) in exon 31 (Figure 2(b)). This transcript was less abundant than the transcript derived from the paternal allele. This aberrantly spliced transcript could not be detected in blood, skin, and lung tissue using RT-PCR.

3.3 | X-chromosome inactivation analyses

X-chromosome inactivation studies performed in peripheral blood DNA revealed an extremely skewed pattern of inactivation in the proband (>90%) and complete skewing in mother (100%). Identification and comparison of the X-chromosomes by the repeat polymorphism in the *AR*-gene revealed the mutated allele to be inactivated in the proband, explaining the absence of the mis-spliced transcript in blood. Likewise, there was also an extremely skewed pattern of inactivation of the mutated X-chromosome in skin and lung tissue of the proband. In heart tissue, however, there was random inactivation with approximately 60% expression of the mutated allele.

4 | DISCUSSION

We describe the clinical and molecular evaluation of two patients, a daughter (proband) and her mother, with terminal osseous dysplasia

FIGURE 1 Phenotype of the proband. (a) Digital fibroma at age 2; (b) Camptodactyly of the distal phalange digit III (box); (c) Brachydactyly of the phalange of digit II (dashed box) and hypoplasia of metacarpal 1 and 2 age 2 (lined box); (d) X-ray of the spine in standing pose at age 3 showing mild flattening of lumbar vertebrae with sinistroconvex lumbal scoliosis with a Cobb's curve of about 25°; (e) computed tomography after IV contrast of the chest (axial [left] and coronal reconstruction [right]), demonstrating diffuse ground glass opacities in all lobes (*). The middle lobe shows destruction of normal architecture, with formation of bullae and bronchiectasis (white arrow). In the lingula there is volume loss with bronchiectasis and formation of smaller bullae (dashed arrow). There is dilatation of the atria and milder dilatation of the left ventricle (∧); (f) MRI-heart (4 chamber cine T2 TRUFI) of mother at age 33 presenting noncompaction cardiomyopathy in end-diastolic phase. Arrow indicating non compact myocardium of the left ventricle. (g) Pedigree of three generations of the family, indicating a TODPD-phenotype (black left side), carriership of the c.5217+5G>C *FLNA* variant (black upper right quadrant) and cardiomyopathy (black lower right quadrant). Men are depicted with squares, women with circles

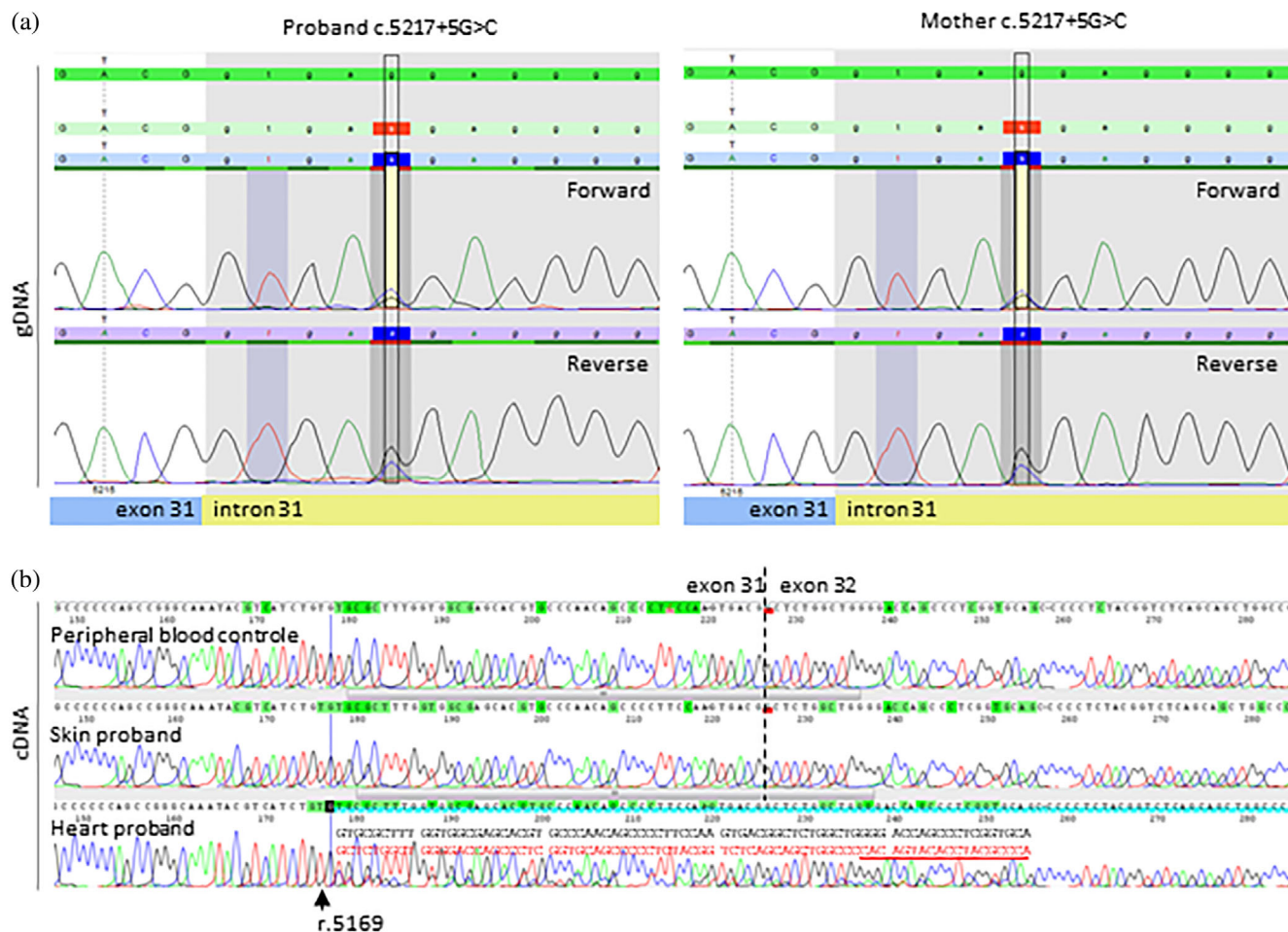


FIGURE 2 Identification and characterization of the variant in *FLNA*. (a) Sanger sequencing of *FLNA* in proband (left) and mother (right) revealed the NM_001110556.1(*FLNA*):C.5217+5G>C variant. (b) Sequence traces of the RT-PCR reactions from (top to bottom): A control (peripheral blood); skin tissue from the proband—also representative for lung tissue and peripheral blood; and heart tissue from the proband. Only in heart tissue from the proband aberrant splicing is present. After nucleotide position r.5169, the frame-shifted and wildtype sequences are superimposed. Above the sequence trace the deduced sequence is shown. The sequence in black shows the normal transcript (part of exon 31) and the red sequence shows the aberrant transcript (part of exon 32 with the position of the reverse primer binding site underlined) resulting in a transcript that is 48 nucleotides shorter, NM_001110556.1(*FLNA*): R.5170_5217del

with pigmentary defects and a novel c.5217+5G>C variant in *FLNA*. This intronic variant is located five nucleotides downstream from the position where the single recurrent c.5217G>A *FLNA* variant occurs that is responsible for all previously reported cases of TODPD. The new variant described here causes identical mis-splicing in exon 31 leading to the deletion of 16 residues in the resulting *FLNA* protein (p.Val1724_Thr1739del). These data further support the contention that this specific deletion is the underlying mechanism leading to the TODPD phenotype. The mis-splicing effect was undetectable in blood of the proband and her mother due to extreme skewing resulting in the inactivation of the maternal (mutated) X-allele, a known phenomenon in TODPD (Sun et al., 2010). This mis-splicing effect could however be demonstrated in affected heart tissue at postmortem. This case reveals a second causative *FLNA*-variant associated with TODPD. Furthermore, it illustrates that splicing analysis in affected tissues can, if available, provide more insight into the pathogenicity of variants in *FLNA*.

We observed a clear variability in phenotypic severity in proband and her mother, the proband being more severely affected than her mother. This is possibly due to a difference in X-inactivation between mother and daughter, where mother has a more extreme X-inactivation pattern than the proband. The nearly complete inactivation of the mutated allele in most tissues could reflect of selection against cells expressing the mutant allele early in development. We were not able to test this in mother because affected tissue (heart) is not available.

In addition to the well-known phenotypic features of TODPD, the proband and mother exhibited restrictive-compaction and non-compaction cardiomyopathy respectively. Although cardiac valvular dysplasia is a known consequence of filaminopathy (OMIM #31440), cardiomyopathy has not been described as a phenotypic feature of TODPD before. Although an alternative pathogenic cause for the cardiomyopathy within this family cannot be fully excluded despite extensive DNA analysis, it is plausible that it could be part of an

extended phenotypic spectrum of TODPD. Segregation analysis of the *FLNA* variant and cardiac evaluation was in accordance with this, although cardiac examination of the noncarrier maternal grandmother could not be performed. Furthermore, the mis-spliced transcript was observed explicitly in heart tissue, where X-inactivation was random and extreme X-inactivation of the mutated allele was absent. Considering the function of *FLNA* as an important player in cross-linking actin—essential for cell shape and motility—(Revenu et al., 2004), a disrupted *FLNA* protein might impact heart-muscle structure and function. Therefore, cardiac screening might be considered in patients with TODPD caused by these two *FLNA* variants.

It is possible that the c.5217+5G>C variant not only leads to the *FLNA* gain-of-function transcript compatible with TODPD, but also to *FLNA* loss-of-function transcripts, since the proband exhibited phenotypic features that are also seen in patients with *FLNA* loss-of-function variants. Childhood interstitial lung disease is a recently recognized clinical consequence of loss-of-function *FLNA* variants (Sasaki et al., 2019). Although we could not confirm the mis-splicing effect in the lung due to extreme skewing of X-inactivation, it might be possible that specific interstitial cell types are principally affected. Epilepsy secondary to periventricular nodular heterotopia is also a common feature in loss-of-function *FLNA* disorders (Wade et al., 2020). PH was not confirmed in our proband as she died before a MRI-scan could be taken and brain autopsy was not performed. If this hypothesis is true, the co-occurrence of these loss-of-function phenotypic features and the TODPD phenotype might be explained by the capability of the c.5217+5G>C variant to produce more transcripts other than the r.5170_5217del transcript that individually confers loss-of-function and gain-of-function. These aberrant transcripts could have been degraded by nonsense mediated mRNA decay (NMD) or have resulted in large PCR fragments or other nonproductive spliceforms that in aggregate result in a reduction in *FLNA* protein and were therefore not detected in our RT-PCR reaction. The r.5170_5217del transcript was less abundant than the transcript derived from the paternal allele. Unfortunately we were not able to test this hypothesis as we do not possess cultures of tissue to inhibit NMD prior to RNA analysis. In general, we propose that, given the exceptional combination of phenotypic features within the OPD-spectrum and the loss-of-function category, physicians should be aware of co-occurring pathology in patients with pathogenic *FLNA* variants.

ACKNOWLEDGMENTS

We are grateful for the contribution of the patient's family to this study. We would like to thank Marloes Willemsen, Maureen Rahanra and Naomi Donner (Academic Medical Centre Amsterdam) for their great technical assistance. We thank Emma Wade and Kaya Fukushima (University of Otago, New Zealand) for helpful discussions. This project has not been funded. The parents of the proband have given informed consent for publication of the medical data and pictures.

CONFLICT OF INTEREST

The authors declare no conflicts of interest.

AUTHOR CONTRIBUTIONS

L. Rumping: Contributed to the concept and design of the study, coordinated the study, wrote the manuscript, contributed to the clinical care of the proband and family. **M.W. Wessels:** Contributed to the concept and design of the study, contributed to the clinical care of the proband and family. **A.V. Postma:** Contributed to the acquisition and interpretation of the data. **J. van Schuppen:** Contributed to the acquisition and interpretation of the data. **M.A. van Slegtenhorst:** Contributed to the acquisition and interpretation of the data. **J.J. Saris:** Contributed to the acquisition and interpretation of the data. **J. P. van Tintelen:** Contributed to the acquisition and interpretation of the data, contributed to the clinical care of the proband and family. **S. P. Robertson:** Contributed to the concept and design of the study. **S. M. Maas:** Contributed to the concept and design of the study, contributed to the clinical care of the proband and family. **R.H. Lekanne Deprez:** Contributed to the concept and design of the study. All co-authors critically revised the manuscript and provided final approval of the manuscript to be published.

DATA AVAILABILITY STATEMENT

The data that support the findings of this study are available on request from the corresponding author. The data are not publicly available due to privacy or ethical restrictions.

ORCID

Lynne Rumping  <https://orcid.org/0000-0002-6427-5033>

Stephen P. Robertson  <https://orcid.org/0000-0002-5181-7809>

REFERENCES

- Allen, R. C., Zoghbi, H. Y., Moseley, A. B., Rosenblatt, H. M., & Belmont, J. W. (1992). Methylation of HpaII and HhaI sites near the polymorphic CAG repeat in the human androgen-receptor gene correlates with X chromosome inactivation. *American Journal of Human Genetics*, 51(6), 1229–1239.
- Bhabha, F. K., Walsh, M., Orchard, D., & Savarirayan, R. (2016). Terminal osseous dysplasia with pigmentary defects; case and brief review of filamin A-related disorders. *The Australasian Journal of Dermatology*, 57(4), 312–315.
- Breuning, M. H., Oranje, A. P., Langemeijer, R. A., Hovius, S. E. H., Diepstraten, A. F., den Hollander, J. C., Baumgartner, N., Dwek, J. R., Sommer, A., & Toriello, H. (2000). Recurrent digital fibroma, focal dermal hypoplasia, and limb malformations. *American Journal of Medical Genetics*, 94(2), 91–101.
- Brunetti-Pierri, N., Lachman, R., Kwanghyuk, L., Leal, S. M., Piccolo, P., van den Veyber, I. B., & Bacino, C. A. (2010). Terminal osseous dysplasia with pigmentary defects (TODPD): Follow-up of the first reported family, characterization of the radiological phenotype, and refinement of the linkage region. *American Journal of Human Genetics*, 152(7), 1825–1831.
- Horii, E., Sugiura, Y., & Nakamura, R. (1998). A syndrome of digital fibromas, facial pigmentary dysplasia, and metacarpal and metatarsal disorganization. *American Journal of Human Genetics*, 80(1), 1–5.
- Landrum, M. J., Lee, J. M., Benson, M., Brown, G. R., Chao, C., Chitipiralla, S., & Maglott, D. R. (2018). ClinVar: Improving access to variant interpretations and supporting evidence. *Nucleic Acids Research*, 46(D1), D1062–D1067.
- Lau, A. W., Brown, C. J., Penaherrera, M., Langlois, S., Kalousek, D. K., & Robinson, W. P. (1997). Skewed X-chromosome inactivation is

- common in fetuses or newborns associated with confined placental mosaicism. *American Journal of Human Genetics*, 61(6), 1353–1361.
- Lek, M., Karczewski, K. J., Minikel, E. V., Samocha, K. E., Banks, E., & Fennell, T. (2016). Analysis of protein-coding genetic variation in 60,706 humans. *Nature*, 536(7616), 285–291.
- Revenu, C., Athman, R., Robine, S., & Louvard, D. (2004). The co-workers of Actin filaments: From cell structures to signals. *Nature Reviews. Molecular Cell Biology*, 5(8), 635–646.
- Robertson, S. P. (2005). Filamin a: Phenotypic diversity. *Current Opinion in Genetics & Development*, 15(3), 301–307.
- Sasaki, E., Byrne, A. T., Phelan, E., Cox, D. W., & Reardon, W. (2019). A review of filamin a mutations and associated interstitial lung disease. *European Journal of Pediatrics*, 178(2), 121–129.
- Sun, Y., Almomani, R., Aten, E., Celli, J., van der Heijden, J., Venselaar, H., & Breuning, M. H. (2010). Terminal osseous dysplasia is caused by a single recurrent mutation in the FLNA gene. *American Journal of Human Genetics*, 87(1), 146–153.
- Wade, E. M., Halliday, B. J., Jenkins, Z. A., O'Neill, A. C., & Robertson, S. P. (2020). The X-linked filaminopathies: Synergistic insights from clinical and molecular analysis. *Human Mutation*, 41(5), 865–883.

How to cite this article: Rumping, L., Wessels, M. W., Postma, A. V., van Schuppen, J., van Slegtenhorst, M. A., Saris, J. J., van Tintelen, J. P., Robertson, S. P., Alders, M., Maas, S. M., & Deprez, R. H. L. (2021). Terminal osseous dysplasia with pigmentary defects and cardiomyopathy caused by a novel FLNA variant. *American Journal of Medical Genetics Part A*, 185A:3814–3820. <https://doi.org/10.1002/ajmg.a.62417>